Three-dimensional Landmarking Based Maxillomandibular Deformity Diagnosis Using Three-dimensional Computer Tomography

Ming-Dar Tsai Wen-Cheng Chung[1] Ming-Shium Hsieh[2,*]

Department of Information and Computer Engineering, Chung Yuan Christian University, Chung-Li, 320, Taiwan, ROC
[1]Oral and Maxillofacial and Dental Department, Taipei Medical University Hospital, Taipei Medical University, Taipei, 110, Taiwan, ROC
[2]Department of Orthopaedics and Traumatology, Taipei Medical University Hospital, Taipei Medical University, Taipei, 110, Taiwan, ROC

Received 21 Apr 2002; Accepted 3 Sep 2002

Abstract

This paper describes a method of automatic maxillomandibular deformity diagnosis based on manipulating volume data constituted of CT slices. This method includes 3D landmarking for diagnosing maxillomandibular deformities by manipulating volume data, measuring distances of landmarks to base planes and classifying the maxillomandibular deformity to determine corresponding surgical modalities, procedures and corrections. A maxilla extrusion example shows, the system equipped with VR simulation functions can provide 3D realistic shaded images to demonstrate 3D landmarks, surgical procedures and prognosis predictions. The comparison between the skull and face before and after surgery shows the surgical plan informed with the computed deformity correction can correct the deformity well.

Keywords: 3D landmarking, Maxillomandibular deformity diagnosis, Surgery treatment, 3D reconstruction

Introduction

Maxillomandibular surgeries are expensive and highly invasive modalities; therefore preoperative evaluations, planning and rehearsal are required and routine. The X-ray based cephalogram is a standard procedure for identifying landmarks on the skull and face [1-4] that are used to evaluate deformities of the skull and face and also compare the difference after surgeries [5,6]. However, two kinds of errors appear in cephalometric procedures: projection errors [7] and identification errors. The latter, especially, appears during identifying the bilateral structures that are important in diagnosing symmetric deformities [8]. Surgical planning and simulation based on the cephalograms can be implemented manually or by computer assisted systems [9-12]. However, such planning and simulation are 2D or 3D wireframe fashion so not realistic.

Current scientific visualization techniques generate realistic (3D shaded) images from a volume constituted of CT or MRI slices. Some computer assisting systems allow clinicians to interactively identify landmarks on the 3D shaded images [13]. Then the systems measure 3D relations among the landmarks to classify deformities and simulate surgical procedures using 3D wireframes (lines connecting the landmarks) to represent the changes of the landmark positions. Such systems can avoid projection errors because volume data resolved interior anatomic structures, but can only reduce not avoid identification errors because of manual landmarking.

In this study, we develop automatic 3D reconstruction methods that identify 3D landmarks, measure the landmarks to classify the deformities and plan surgical procedures to correct the maxillomandibular deformities. The surgical procedures are then simulated by our VR surgical simulator [14-16]. The simulation results can impress surgeons that will occur during operations. The 3D identification of landmarks and 3D evaluation of surgical plans with the verification of the VR surgical simulations can achieve an accurate and versatile diagnosis and surgical planning for the maxillomandibular deformity.

* Corresponding author: Ming-Shium Hsieh
Tel: +886-2-27372181 ext. 3118; Fax: +886-2-27375618
E-mail: shiemin@tmu.edu.tw

Methods

3D landmarking by 3D CT data

Fig. 1 illustrates the landmarks being defined in our system. Most of them are similar to the definitions as in the traditional cephalogram but with little modification because a volume constituted of CT slices can provide 3D positions. However, the coordinate system of the skull is not identical to

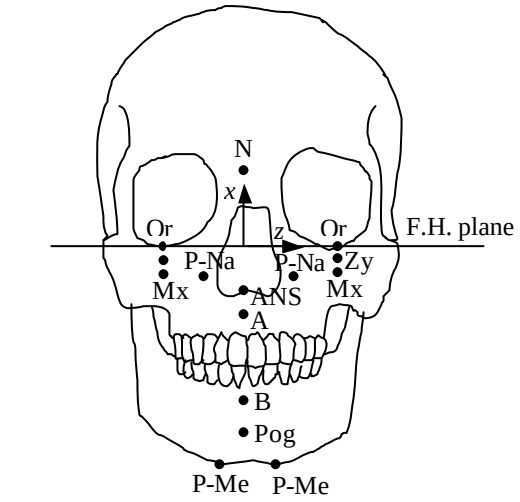

(A) Frontal view

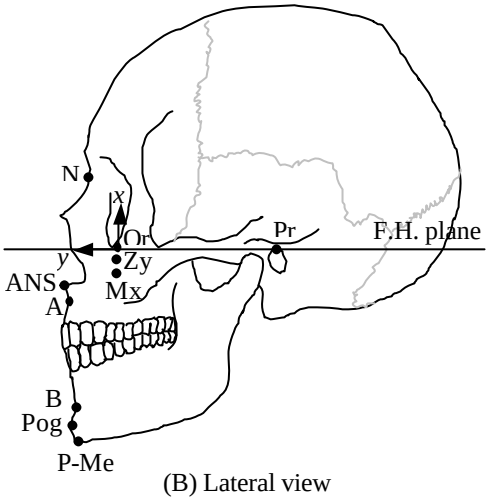

(B) Lateral view

Figure 1. Landmarks for diagnosing maxillomandibular deformities

Figure 2. Implementation of landmarking and surgical simulation under VR environment

the volume coordinate system, determination of a primary plane for positioning the skull coordinate system is required. The resulting primary planes of the skull coordinate system are usually near parallel to the primary plans of the volume coordinate system but not identical. In the paper, *X, Y, Z* mean coordinates of the volume coordinate system, while *x, y, z* mean the coordinates of the skull coordinate system.

Or (L/R) and Pr (L/R) are identified interactively to determine a primary plane, Frankfort Horizontal plane. Because Frankfort Horizontal plane means the horizontal of the skull, it is easily identified and verified by clinicians' observation. Other landmarks and primary planes are automatically determined by the following algorithms. The landmarks with L/R mean bilateral structures that are symmetric pairs about the center plane of the skull.

(1) Or(L/R) and Pr (L/R)

Or represents the bottom of the orbital bone. Pr represents the porion. As Fig. 2 shows, a clinician wearing a shuttle eyeglass is identifying these four landmarks on stereographic images (a pair of 3D images for two eyes respectively).

(2) F.H. plane

In the traditional cephalogram, Frankfort Horizontal plane (F.H. plane) is a line connecting Or and Pr. Our system uses Or(L/R) and Pr(L/R) to approximate the F.H. plane by solving a linear equation system with the least square approximation [17]. If the F.H. plane is represented as $aX+bY+cZ=d$ in the volume coordinate system, and the coordinates of Or(L), Or(R), Pr(L) and Pr(R) are as follows:

$$\text{Or(L)} = (X_1, Y_1, Z_1)$$
$$\text{Or(R)} = (X_2, Y_2, Z_2)$$
$$\text{Pr(L)} = (X_3, Y_3, Z_3)$$
$$\text{Pr(R)} = (X_4, Y_4, Z_4)$$

Then we can obtain a system of linear equations, $AW = B$

$$A=\begin{bmatrix} X_1 & Y_1 & Z_1 \\ X_2 & Y_2 & Z_2 \\ X_3 & Y_3 & Z_3 \\ X_4 & Y_4 & Z_4 \end{bmatrix}, \quad W=\begin{bmatrix} a \\ b \\ c \end{bmatrix}, \quad B=\begin{bmatrix} d \\ d \\ d \\ d \end{bmatrix}$$

Then, the best-approximated W can be determined by the following equation.

$$A^{\mathrm{T}} AW = A^{\mathrm{T}} B$$

As Fig. 3 shows, the F.H. plane is the *yz*-plane of the skull coordinate system, its surface normal is the *x*-axis, the origin is the midpoint of the two projections of Or (L/R) on the F.H. plane, and the *z*-axis is the direction from the origin to the projection of Or(L). The *xy*-plane is also called the center plane of the skull. The F.H. plane and the coordinate system can be re-determined by re-identifying either of Or(L/R) and Pr (L/R) if the clinician considers the current F.H. plane is not a good choice.

(3) N and Me

N (Nasion) is the most frontal point on the fissure between the nasal and frontal bone of the center (*xy*-) plane (Fig. 4(A)). Me (maximum extremal mandible) is also on the *xy*-plane and the most distal point of the mandible. In our system, the landmarks on the *xy*-plane are all located on the

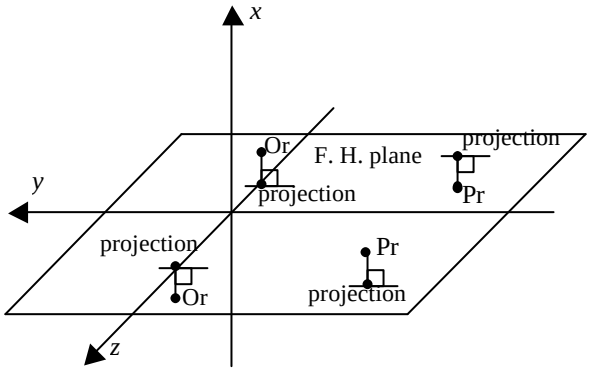

Figure 3. Skull coordinate system and Frankfort Horizontal plane best approximated by Or(L/R) and Pr(L/R)

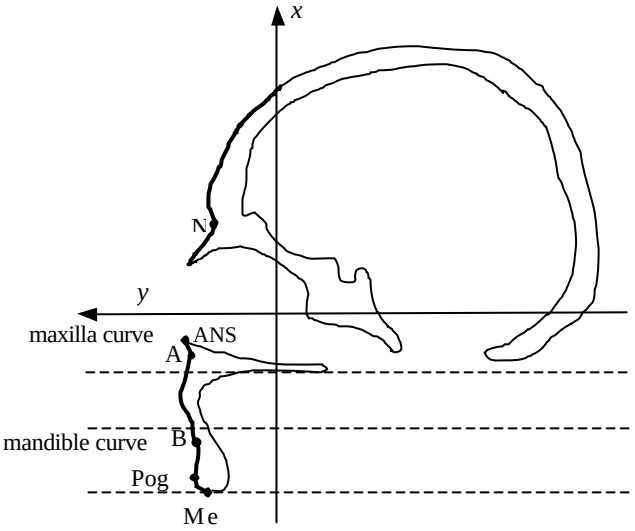

(a) Landmarks on the center plane

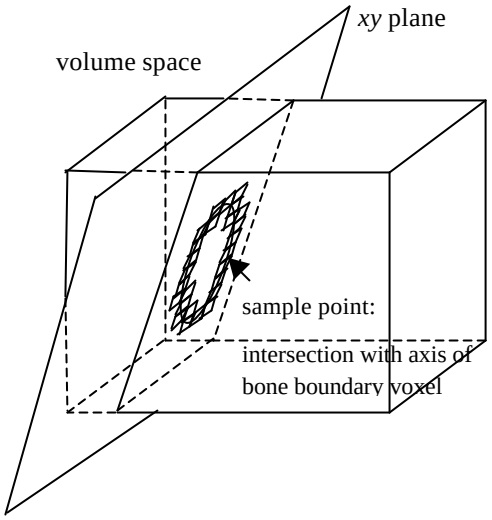

(b) Bone profile connected by intersections of *xy* plane with axes of bone boundary voxels

Figure 4. Landmarking on center plane of skull

outmost profile of bones. The bone boundaries (profiles) can be obtained by connecting sample points of bones. Every sample point is an intersection of the *xy*-plane with an axis of

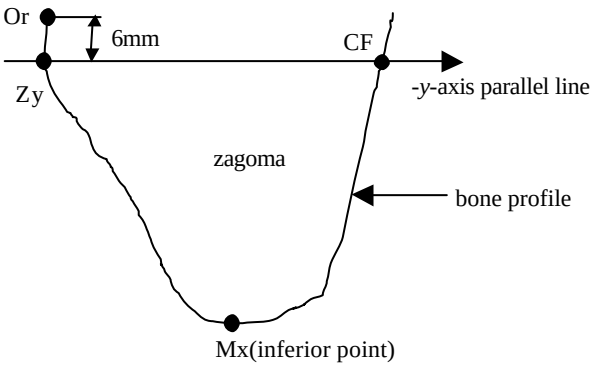

Figure 5. Landmarking on zagoma using an *xy*-plane parallel plane to intersect with zagoma

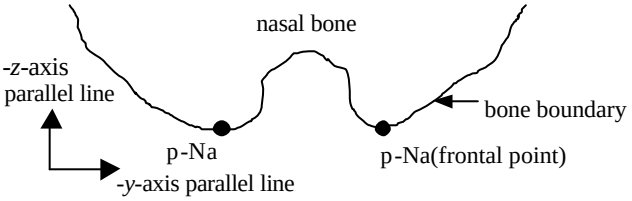

Figure 6. Landmarking on zagoma using a *yz*-plane parallel plane to intersect with nasal bone

a bone-boundary voxel defined as any of its six neighboring voxels does not belong to bone [14] (Fig. 4(B)). We use a cubic polynomial $y=f(x)=ax^3+bx^2+cx+d$ to approximate the outmost profile of bones on the $+x+y$ region of the *xy*-plane (Fig. 4(A)); meanwhile, *a*, *b*, *c* and *d* are determined by interpolating the outmost sample points with the least square approximation [18]. The outmost sample points are those with the largest *y*-value corresponding to each *x* integer coordinate. Then, N is the local minimum of the outmost profile, in which $f'(x)=0$ and $f''(x)>0$. Me is the most inferior point of the outmost profile of bone at the $+x$-y region of the *xy*-plane (Fig. 4(A)), meaning that it is the sample point with the smallest *x* coordinate. The outmost profile at the $+x$-y region (from the origin to the smallest *x* coordinate) can be divided as three parts, the inferior part is called as the mandible curve and the superior is the maxilla curve.

(4) A, B, Pog and ANS

A is the local minimum of the maxilla curve (Fig. 4(A)), therefore can be determined by the similar method of using a cubic polynomial to approximate the maxilla curve and then determine the local minimum. B is the local minimum of the mandible curve (Fig. 4(A)), therefore can be determined by using a cubic polynomial to approximate the mandible curve and then determine the local minimum. Pog, the pogonion, is the local maximum of the mandible curve. ANS represent the frontal point of the anterior nasal bone; therefore it is on the maxilla curve and has the largest *x* value.

(5) Mx(L/R)

We define Mx(L/R) as the most inferior point on the zagoma under Or(L/R). Therefore, Mx(L) is a sample point

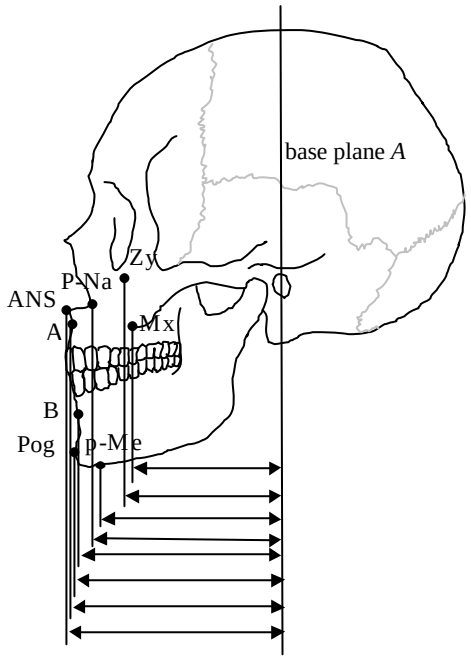

(a) Measurements for diagnosing extrusion or protrusion deformities

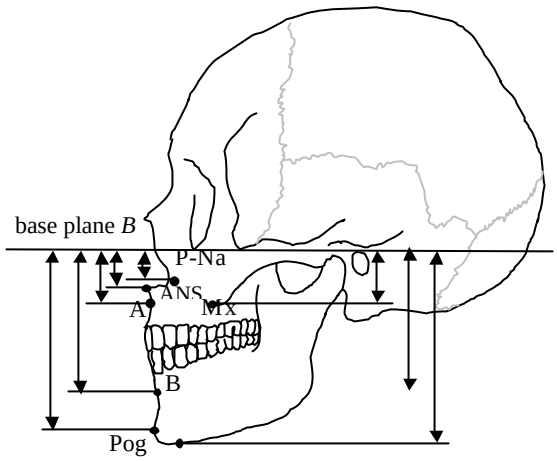

(b) Measurements for diagnosing excess or insufficient deformities

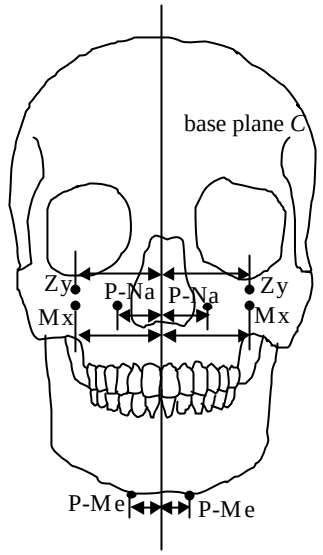

(c) Measurements for diagnosing symmetric deformities

Figure 7. Measurement for diagnosing maxillomandibular deformities

with the smallest *x* coordinate from the intersections of axes of bone-boundary voxels with the plane parallel to the *xy*-plane and passing Or(L) (Fig. 5). Similarly, Mx(R) is sample point with the smallest *x* coordinate from the intersections of axes of bone-boundary voxels with the plane parallel to the *xy*-plane and passing Or(R).

(6) Zy(L/R) and CF(L/R)

We also define Zy(L/R) and CF(L/R) from the bone surface of the zagoma (Fig. 5). A line that is 6mm under Or(L/R) and parallel to the -y-axis determines them. Algorithms of line traversal in a volume can determine the voxels that a line has traversed [19,20]. Two bone-boundary voxels and then two sample points on the zagoma will be traversed by the line. The one directly under Or(L) or Or(R) is Zy(L) or Zy(R). The other one is CF(L/R).

(7) p-Na (L/R)

We define p-Na(L/R) (L/R para Nasal bone) as the frontal point of bone boundary on a plane that is parallel to the *yz*-plane and 1mm above the ANS (Fig. 6). P-Na(L/R) are the intersections (sample points) of axes of bone-boundary voxels with the plane. The intersection with *z* value and the largest *y* value is P-Na(L) and the one with -*z* value and the largest *y* value is P-Na(R).

(8) p-Me(L/R)

We define P-Me(L) (Left para Mentum) as the sample point of bone boundary with the smallest *x* value in the $-x+y+z$ region, while P-Me(R) (Right para Mentum) has the smallest *x* value in the $-x+y+z$ region. We use planes that parallel to the *yz* plane and near Me to intersect with bones. By comparing the *x* and *y* coordinates of the intersections of axes of bone-boundary voxels with the planes, P-Me(L/R). The two intersections (p-Me(L/R)) with the smallest *x* values can be determined.

Deformity measurement, classification and surgical planning

The primary planes of the skull coordinate system determine the base planes for diagnosing maxillomandibular deformities. As Fig. 7 shows, the base plane *A* is parallel to the *xz*-plane and passes the midpoint of Pr(L/R). *A* is used to measure anteroposterior distances of landmarks and such detect deformities of extrusions and protrusions of the skull (Fig. 7(A)). The base plane *B* is the *yz*-plane and used to measure perpendicular distances of landmarks and such detect deformities of excess and insufficiency (Fig. 7(B)). The base plane *C* is the *xy*-plane and used to measure horizontal distances of landmarks and such detect deformities of symmetry (Fig. 7(C)).

Therefore, three kinds of deformities can be determined from the measured distances to the three base planes. Regarding the maxilla deformities, the measured distances from the landmarks, ANS, A, Mx, Zy and p-Na to the base plane *A* determine the deformities about the anteroposterior extrusion and protrusion of the skull. The measured distances from ANS, A, Mx and p-Na to the base plane *B* determine the

Table 1. Maxillomandibular deformity classification by measuring distances from landmarks to base planes

	base plane *A*														base plane *B*														base plane *C*												
	ANS	A	Mx		Zy		p-Na		CF		B	Pog	p-Me		ANS	A	Mx		Zy		p-Na		CF		B	Pog	p-Me		ANS	A	Mx		Zy		p-Na		CF		B	Pog	p-Me		occlusion
			L	R	L	R	L	R	L	R			L	R			L	R	L	R	L	R	L	R			L	R			L	R	L	R	L	R	L	R			L	R	condition
Class II,division 1 deformity with normal overbite											-	-	-	-																												normal overbite
Class II,division 1 deformity with deep bite											-	-	-	-																												deep bite
Class II,division 1 deformity											-	-	-	-																												
Vertical maxillary excess without open bite															-	-	-	-	-	-	-	-	-	-																		open bite
Class II deformity with open bite											-	-	-	-																												open bite
Mandibular prognathism											+	+	+	+																												
Maxillary deficiency	-	-	-	-	-	-	-	-							-	-	-	-	-	-	-	-	-	-						-	-											
Class III deformity with open bite											+	+	+	+											+	+	+	+														open bite
The midface dentofacial deformity	-	-	-	-	-	-	-	-							+	+	+	+	+	+	+	+	+	+																		
Bimaxillary protrusion with or without open bite	+	+					+	+			+	+																														
Class I vertical maxillary excess with or without open bite	+	+	+	+	+	+	+	+	+	+	+				+	+	+	+			+	+																				
Transverse maxillary deficiency																														-	-											
Asymmetric Class II dentofacial deformity											-	-	-	-															-/+	-/+							-/+	-/+	-/+	-/+	
Asymmetric Class III dentofacial deformity											+	+	+	+															-/+	-/+							-/+	-/+	-/+	-/+	

(+: measured distance is excess comparing to normal people, - : measured distance is insufficient comparing to normal people)

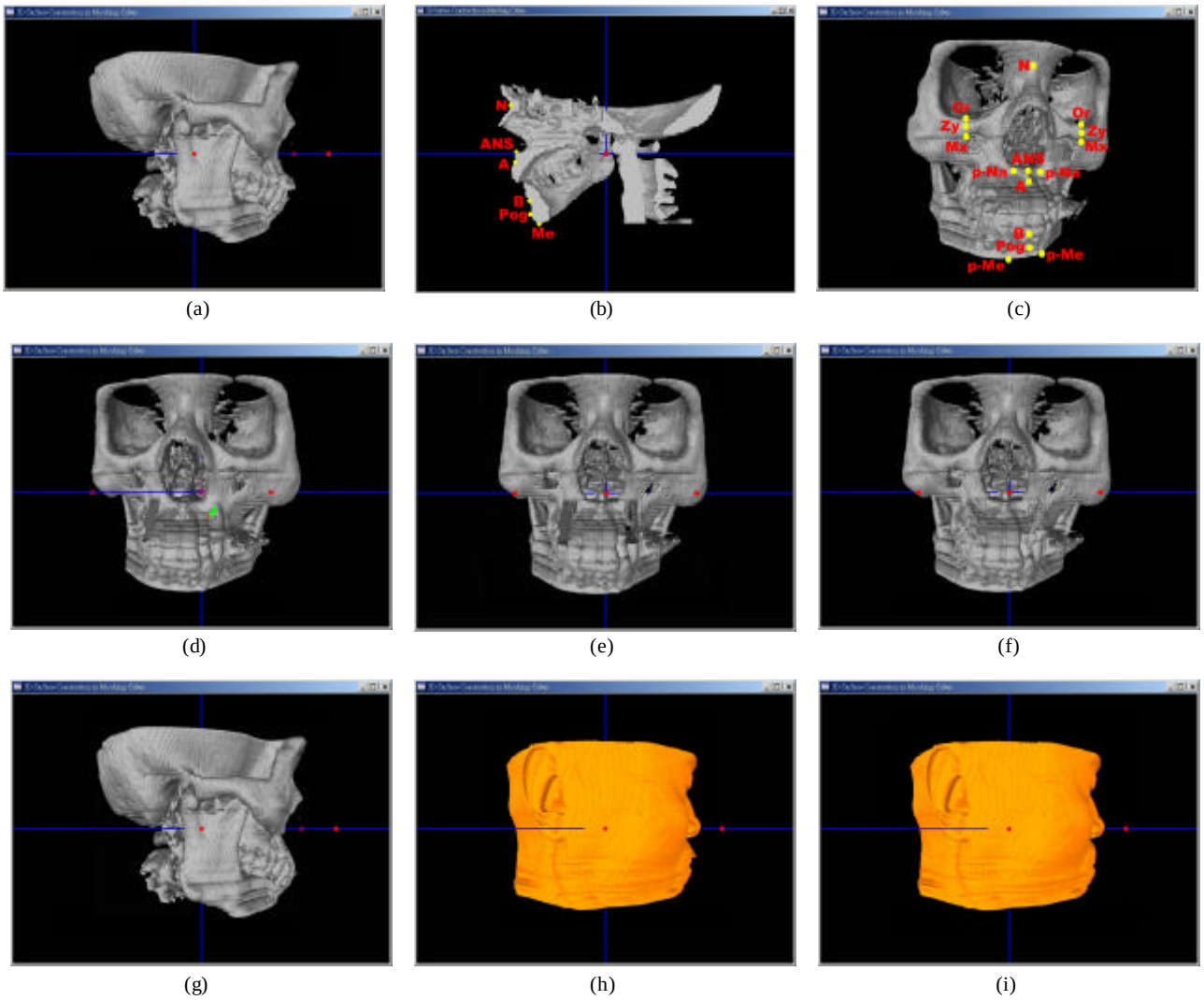

Figure 8. Maxilla extrusion example of maxillomandibular deformity diagnosis and surgical simulation (a): Lateral view with identified Pr(R); (b): Identified landmarks on center plane of skull, (c): Near frontal view with identified landmarks, and right premolar is been cutting; (d): Right premolar has been sectioned to be separate and removed, and left premolar is been cutting; (e): Left premolar has been cut away and the maxilla has also been cut to be separate and repositioned; (f): Maxilla and skull have been fused together; (g): Lateral view after the fusion; (h): Lateral view of face before surgery; (i): Lateral view of face after healing.

deformities of the perpendicular excess and insufficiency. Then, the measured distances from Mx, Zy and CF and p-Na to the base plane *C* determine the deformities of the symmetry about the center plane.

Regarding the mandible deformities, the measured distances from the landmarks *A*, Pog and p-Me to base determine the deformities of the anteroposterior extrusion and protrusion. The measured distances from B, Pog and p-Me to the base plane *B* determine the deformities of the perpendicular excess and insufficiency. Then, the measured distances from p-Me to the base plane *C* determine the deformities of the symmetry about the center plane.

Table 1 shows the classification of 14 types of maxillomandibular deformities determined from the measured distances. Excess or insufficiency of the distances, comparing to the values of normal peoples, classifies some deformity. Surgical modalities corresponding to the classified deformity are determined followed [21]. The measured excess or insufficiency of the distances from the base planes to the landmarks is also used as the correction in the surgical procedures.

Simulation of the surgical planning

Surgical procedures of osteotomy for correcting the 14 types of maxillomandibular deformities are then simulated by our reported simulator [14-16]. The simulation system uses a voxel structure to represent the surface topology and geometry of an anatomic structure. In this data structure, a voxel has 6 face-flags and distance-levels that can be used to improve rendering speed and quality and enables the closure check for the intersections of swept surfaces of surgical tools and anatomic structures, and thus makes various manipulations on separate anatomic structures feasible. The simulation results of every procedure of the surgical modalities can be used to impress surgeons to show how a bone is opened, corrected and closed.

Results

Fig. 8 shows the rendering results of a corrective osteotomy that was performed to correct a maxilla extrusion. The volume has a resolution of 256×256×54. Fig. 8(A) shows a lateral-view skull before simulation; in which an open bite deformity can be observed. The landmark of Pr(R) was also interactively identified. After Pr(L/R) and Or(L/R) were interactively identified, all the landmarks and based planes were identified. Fig. 8(B) shows the identified landmarks on the *xy*-plane. Fig. 8(C) shows a near frontal view in which the landmarks are also demonstrated. Tab. 2 shows the measurements from the landmarks to the base planes, the classified deformity and the corresponding surgical treatment including the surgery and prognosis plans [21].

Fig. 8(C) also shows a virtual tool is cutting the right premolar. Fig. 8(D) shows a virtual tool is cutting the left premolar, and also shows the right premolar has been cut away by rectangular cuts on the maxilla to form a separate structure followed by removing the separate rectangular premolar. Fig. 8(E) shows the left premolar was also cut away, and the maxilla became separate and has been repositioned 1mm upward and 10mm backward corresponding to the computed correction. Fig. 8(F) shows the maxilla and the skull had been fused together in which bone voxels were generated inside the right and left premolar caves. Fig. 8(G) shows the lateral view after the fusion predicting the prognosis after several months of the surgery. Comparing the 3D images of the skull before and after the simulations (in Fig. 8(A) and 8(G)), this osteotomy demonstrated to be a feasible means of correcting the maxilla extrusion.

Our simulation system automatically determines, repositions associated soft tissues and heal up the associated soft tissues with original soft tissues as the ways for rigid bones. Fig. 8(H) and 8(I) show the faces of lateral views before surgery and after the healing respectively. Comparing to the faces before and after surgery reveals that the osteotomy could also obtain natural face morphology.

Discussion

In this study, we manipulate volume data to automatically identify base planes and landmarks for diagnosing maxillomandibular deformities. By measuring distances of the landmarks to the base planes, deformity classification and corrections in surgery plans can be automatically computed to avoid manual errors. The new tool, combining with surgical simulation may facilitate automated diagnosis, surgical planning and verification, prognosis assessment and management of patients with maxillomandibular deformities. The accurate preoperative evaluation, intraoperative uncertainty deletion and precise postoperative assessments can be expected.

Comparing to the related methods that identify and measure 2D landmarks and simulate surgery in 2D or 3D wireframe fashions, our identification, measurement and simulation are all 3D and demonstrate with 3D realistic shaded images. Comparing to other 3D volume manipulation methods, our method are automatic and can be virtual reality (with stereographic images) fashion to provide not only landmark identification and measurement but also simulation of procedures and prediction of prognosis.

However, learning to use simulation functions to simulate the osteotomic procedures is necessary. Because the maxillomandibular deformity correction is not only functional but also aesthetic problems, surgeons have to communicate with each other or with the patients through the virtual reality simulator and then select a modality from possible ones or determine the corrections in procedures for correcting the deformity. How to integrate the opinions of oral and maxillofacial and plastic surgeons and patients with the system-computed results seems a future topic.

More measurements or landmarks or quantification of landmark measurements may be required. For example, the ambiguities between some classifications such as *Class II division I, with deep bite* or *with normal overbite* and *Class II with open bite* are all caused by insufficiency of the measurements from B, Pog and PMe to the base plane *A* (Table 1) Therefore, more measurements are needed for further classification.

Three-dimensional reconstruction has an inherent advantage of possessing 3D and interior anatomic information, however has a resolution problem. CT slices with a short enough interval are usually not practiced in real cases. This problem does not affect the calculations about the landmarks and measurements, but may lower the quality of 3D images. Too poor 3D images may lower the accuracy when interactively identifying Or(L/R) and Pr (L/R) and simulating surgery. Interpolation that increases the number of slices can improve the quality of 3D images. The insufficient resolution may also lose anatomic information; for example, few slices resolving the teeth usually cannot reveal the occlusion. Such problem can be solved by 2D manually bordering on slices or by using surgical functions to border the anatomy on 3D images. As the example shown in Fig. 8, we have sectioned the teeth to enable the upper teeth moving together with the maxilla.

This study suggests that similar methods may be applied with few modifications to other anatomic structures of musculoskeletal system such as craniofacе and hip etc.

Conclusion

This study revealed identification of landmarks by volume data was accurate and reliable because of volume inheritance of resolving 3D interior anatomic structures. By manipulating volume data, automatic identifications and measurements of landmarks for evaluating and classifying maxillomandibular deformities were developed. These landmarks include Frankfort horizontal plane, nasion, extremal mandible, local minimum of maxilla, local minimum and maximum of mandible, anterior nasal bone, most inferior zagoma, zagoma under orbital, paranasal bone, mentum and para mentum. Through the verification of VR surgical simulations, we confirmed that the deformity could be corrected with the surgical plan based on the automatic classification by the automatic landmarking.

Table 2. Measurement results and treatment plan

Measurements for diagnosing maxilla

	ANS	A	MX		Zy		p-Na		CF	
			L	R	L	R	L	R	L	R
base plane *A*	95.1	92.9	71.2	71.8	85.4	86.1	79.4	48.3	*****	*****
base plane *B*	43.5	50.3	48.4	47.9	*****	*****	39.3	40.1	*****	*****
base plane *C*	*****	*****	30.1	29.9	40.5	41.2	20.2	19.9	40.5	41.2

in mm

Measurements for diagnosing mandible

	B	Pog	p-Me	
			L	R
base plane *A*	? 82.1	? 84.3	? 112.4	? 115.1
base plane *B*	? 85.3	? 88.5	120.3	119.4
base plane *C*	*****	*****	14.3	14.9

in mm

? : measured distance is insufficient comparing to normal people.

Classified deformity: *Class II, division I deformity with openbite*

Surgical treatment

Presurgical orthodontic treatment
1. Extract lower first premolars
2. Place lower appliances
3. Retract lower canines
4. Begin lower incisor retraction; extract upper first premolars
5. Place upper appliances; align and level segmentally
6. Ideal lower arch and ideal upper sectional arches
7. Impression for feasibility model surgery

Orthognathic surgery
1. Modified total subapical superior maxillary repositioning
2. Surgical control of nasal and upper lip esthetics
3. Augmentation genioplasty

Postsurgical orthodontic treatment
1. Check appliances; repair as necessary
2. Continuous coordinated upper arch; stabilizing lingual arch
3. Elastics as necessary
4. Routine finishing procedures
5. Retain

Acknowledgment

The authors would like to thank the National Science Council for financial support of this research under grant numbers NSC-89-2213-E-033-070.

References

[1] H. Hofrath, "die Bedeutung der Roentgenfer-und Abstandsaufnahme fuer die Diagnostik der Kieferanomalien", *Fortschr Orthod*, l:34-41, 1931.

[2] S. S. Bhitia, and J.H. Sowray "A Computer-aided design for orthonathic surgery", *Bristich Journal of Oral and Maxillofacial Surgery*, 22:237-253, 1984.

[3] E.K. Pae, GA. McKenna, T.J. Sheehan, R. Garcia, A. Kuhlberg and R. Nanda, "Role of lateral cephalograms in assessing severity and difficulty of orthodontic cases", *American Journal of Orthodontics & Dentofacial Orthopedics*, 120(3): 254-262, 2001.

[4] N.S. Raju, K.G. Prasad and V.P. Jayade,"A modified approach for obtaining cephalograms in the natural head position", *Journal of Orthodontics*, 28(1): 25-28, 2001.

[5] Y.T. Chen, K.S. Cheng, M.L. Chien and Liu, L.K., "Feature Curves Based Cephalometric Superimposition", *Joumal of Medical and Biology Engineering*, 20: 211-218, 2000.

[6] N. Higurashi, M. Kikuchi, S. Miyazaki and Y. Itasaka, "Comparison of ricketts analysis and Downs-Northwestern analysis for the evaluation of obstructive sleep apnea cephalograms", P*sychiatry & Clinical Neurosciences*, 55(3):259-260, 2001.

[7] S. Baumrind, F. Moffit and S. Curry , "The geometry of three-dimensional measurement from paired coplanar X-Ray images", *Am. Journal Orthod.*, 84:313-326, 1983.

[8] W.J. Moorrees et al., "Growth of the facial skeleton in the Hominoidea", *New Year Academic Press*, 1974.

[9] B.S. Savara, "Biostereometrics and computer graphics for patients with craniofacial maoflomations: Diagnosis and treatment planning", *Plast Teconstr Surg*, 75: 495-530, 1985.

[10] F.L. Bookstein, B. Grayson, C.B. Cutting, H.C. Kim and J.G. McCarthy, "Landmarks in Three Dimensions: Reconstruction from cephalograms versus direct observation", *Am. Journal Orthod. Dentofac. Orthop.*, 133-140, 1991.

[11] T.G. Kwon, Y. Mori, K. Minami, S.H. Lee and M. Sakuda, "Stability of simultaneous maxillary and mandibular osteotomy for treatment of class III malocclusion: an analysis of three-dimensional cephalograms", *Journal of Cranio-Maxillo-Facial Surgery*, 28(5):272-277, 2000.

[12] T. Stamm, H.A. Brinkhaus, U. Ehmer, N. Meier and F. Bollmann, "Computer-aided automated landmarking of cephalograms", *Journal of Orofacial Orthopedics*. 59(2):73-81, 1998.

[13] I. Ono, T. Ohura, E. Narami, K. Kawashima, I. Matsuno, S. Nakamura, N. Ohhata, Y. Uchiyama, Y. Watanabe, F. Tanaka and T. Kishinami, "Three-dimensional analysis of craniofacial bones using three-dimensional computer tomography", *Journal of Cranio-Maxillo-Facial Surgery*, 1992, Vol. 20, pp. 49-60.

[14] M.D. Tsai, M.S. Hsieh and S.B. Jou, "Virtual reality orthopedic surgery simulator", *Comput. Biol. Med.*, 31(5): 333-351, 2001.

[15] M.D. Tsai, S.B. Jou and M.S. Hsieh, "Accurate surface voxelization for manipulating volumetric surfaces and solids with application in simulating musculoskeletal surgery", in Pacific Graphics, *IEEE CS*, October 2001, 234-243.

[16] M.S. Hsieh, M.D. Tsai and W.C. Chung, "Virtual reality simulator for osteotomy and fusion involving the musculoskeletal system", *Comput. Med. Imag. Grap.*, 26(2): 91-101, 2002.

[17] H. Anton and C. Rorres, "Best Approximation", In: Elementary linear algebra, ch.6: 328-337, 1994.

[18] W. Cheney and D. Kincaid, "Smoothing of data and the method of least squares", In: Numerical Mathematics and Computing, Brooks/Cole(Eds.), ch.10: 381-409, 1994.

[19] M.D. Tsai and M.S. Hsieh "Surface rendering for multi-axial cross sections", *Journal of Information Science and Engineering*, 17(1): 113-132, 2001.

[20] D. Cohen and A. Kaufman, "3D line voxelization and connectivity control", *IEEE CG&A*, 17: 80-87, 1997.

[21] R.J. Fonseca, and S.B. Baker, "Oral and Maxillofacial Surgery "; In: Wolford left/Craniofacial/Cosmetic Surgery, 1st ed, W.B. Saunders Company. U.S.A., 6: 149-533, 2000.